A Highly Linear Temperature Sensor Operating up to 600°C in a 4H-SiC CMOS Technology

Mo, Jiarui; Li, Jinglin; Zhang, Yaqian; Romijn, Joost; May, Alexander; Erlbacher, Tobias; Zhang, Guoqi; Vollebregt, Sten

DOI
10.1109/LED.2023.3268334

Publication date
2023

Document Version
Final published version

Published in
IEEE Electron Device Letters

A Highly Linear Temperature Sensor Operating up to 600°C in a 4H-SiC CMOS Technology

Jiarui Mo, *Graduate Student Member, IEEE*, Jinglin Li, Yaqian Zhang, *Student Member, IEEE*, Joost Romijn, *Member, IEEE*, Alexander May, Tobias Erlbacher, Guoqi Zhang, *Fellow, IEEE*, and Sten Vollebregt, *Senior Member, IEEE*

***Abstract*— In this work, a highly linear temperature sensor based on a silicon carbide (SiC) p-n diode is presented. Under a constant current biasing, the diode has an excellent linear response to the temperature (from room temperature to 600°C). The best linearity (coefficient of determination R^2 = 99.98%) is achieved when the current density is 0.53 mA/cm^2. The maximum sensitivity of the p-n diode is 3.04 mV/°C. The temperature sensor is fully compatible with Fraunhofer Institute (FHG) IISB's open SiC CMOS (complementary metal-oxide-semiconductor) technology, thus enabling the monolithic integration with SiC readout circuits for high-temperature applications. The sensor also features a simple fabrication process. To our knowledge, the presented device is the first SiC diode temperature sensor that does not require a mesa etch or backside contacts.**

***Index Terms*— Silicon carbide, p-n diode, temperature sensor, high temperature.**

I. Introduction

THE demand for high-temperature monitoring is increasing rapidly in industries, such as oil drilling, automotive, and aerospace [1], [2]. Despite the fact that people have developed various advanced temperature sensors with mature silicon (Si) technology, accurate temperature sensing above 200°C is still a very challenging task [3], [4], [5]. Silicon carbide (SiC) is considered a promising wide bandgap (WBG) semiconductor for temperature sensing in harsh environments [1], [2]. Thanks to its large bandgap (E_g = 3.26 eV), SiC electronics can, in theory, work up to 1000°C [6]. To date, the most common implementation of a SiC temperature sensor is based on different diodes due to their simplicity and robustness.

Manuscript received 21 March 2023; revised 9 April 2023; accepted 14 April 2023. Date of publication 19 April 2023; date of current version 23 May 2023. This work was supported by the intelligent Reliability 4.0 (iRel40) European Co-Funded Innovation Project through the Electronic Components and Systems for European Leadership (ECSEL) Joint Undertaking (JU) under Grant NO876659. The review of this letter was arranged by Editor D. Hisamoto. *(Corresponding authors: Jiarui Mo; Sten Vollebregt.)*

Jiarui Mo, Jinglin Li, Yaqian Zhang, Joost Romijn, Guoqi Zhang, and Sten Vollebregt are with the Electronic Components, Technology and Materials (ECTM) Group, Department of Microelectronics, Delft University of Technology, 2628 CD Delft, The Netherlands (e-mail: J.Mo@tudelft.nl; S.Vollebregt@tudelft.nl).

Alexander May and Tobias Erlbacher are with the Fraunhofer Institute for Integrated System and Devices Technology (IISB), 91058 Erlangen, Germany.

Color versions of one or more figures in this letter are available at https://doi.org/10.1109/LED.2023.3268334.

Digital Object Identifier 10.1109/LED.2023.3268334

However, most of the reported SiC diode-based temperature sensors have a maximum temperature limit of less than 600°C [7], [8], [9], [10], [11], [12], [13]. Zhang et al. reported the highest operating temperature so far (up to 600°C) [14]. However, the sensor has relatively poor linearity, and therefore it will require intensive calibration in practical use. Additionally, from a measurement system point of view, it is desirable to monolithically integrate the sensor with readout electronics to enhance the signal-to-noise ratio (SNR) and reliability [15]. Nevertheless, past sensor designs have yet to considered whether a sensor is compatible with an integrated circuit (IC) technology [7], [8], [9], [10], [11], [12].

In this letter, we report a SiC p-n diode temperature sensor in a 4H-SiC CMOS technology provided by FHG IISB. The temperature sensor uses the existing layers in the CMOS process, ensuring full compatibility with the planar SiC CMOS circuits. SiC MOSFET characterization and digital and analog ICs based on this SiC CMOS process were reported elsewhere [16]. The device was characterized from room temperature to 600°C, showing excellent sensitivity and linearity.

II. SiC CMOS Technology and Device Structure

The SiC CMOS process was carried out on 350 μm thick 4-inch 4H-SiC wafers. The surface orientation is 4° off-axis (0001) for better epitaxial growth. A 9 μm nitrogen-doped epitaxial layer with a concentration between 5×10^{14} and 8×10^{14} atoms/cm^3 was grown, where the implantation of n-well (NW), p-well (PW), shallow-p (SP), and shallow-n (SN) layers were followed, with doping concentration of 5×10^{15}, 1×10^{17}, 4.5×10^{19}, and 3.5×10^{19} atoms/cm^3. The activation of dopants was done with a 30-minute annealing step at 1700°C in an argon flow. After the growth of gate oxide, a nitric oxide (NO) annealing was performed for 60 minutes at 1300°C to reduce the interface state density. Then, poly-Si was deposited and patterned as the gate. NiAl and Ti/Al were applied in the contact openings for n-type and p-type contacts, and were annealed in argon at 980°C for 2 minutes to form silicide. Finally, a stack of Ti/Al/Ti (50/700/20 nm) was used as the metal layer. The Ti below the Al serves as an adhesion layer and barrier to prevent Al diffusion into SiO_2.

As shown in Figure 1, the p-n diode-based temperature sensor consists of PW and SN in the CMOS technology. An additional SP region was defined in the PW to form a better p-type contact with Ti/Al at the anode. Figure 2 shows an image of the temperature sensor under an optical microscope.

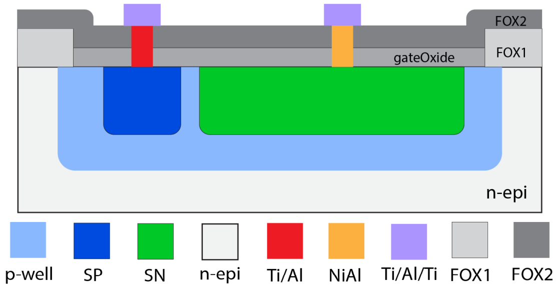

Fig. 1. A cross-sectional view of the diode in the CMOS process.

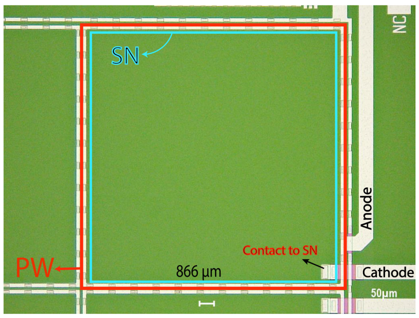

Fig. 2. An optical microscopic image of the p-n diode. The SN layer is implanted in the PW layer. The PW layer is encircled by an SP guard ring and the metal layer for p-type ohmic contact.

The metallurgical area of the p-n junction is around 0.75 mm^2 (866 μm $\times$ 866 μm).

III. Measurement and Discussion

A. p-n Diode Sensing Principle

The forward voltage of a p-n diode (V_F) under a constant biasing current (I_{bias}) can be described by:

$$V_F = nkT/q \cdot \ln(I_{bias}/AJ_0) \tag{1}$$

where n is the ideality factor of the diode, k is the Boltzmann constant, T is the absolute temperature, q is the elementary charge, A is the area of the metallurgical junction, and J_0 is the reverse saturation current density. The temperature-dependency of V_F, i.e., the sensitivity of the diode temperature sensor S, can be obtained from the first derivative of V_F:

$$S = \frac{dV_F}{dT} = \frac{nk}{q}\ln\left(\frac{I_{bias}}{AJ_0}\right) + \frac{nkT}{q}\cdot\frac{d[\ln(I_{bias}/AJ_0)]}{dT} \tag{2}$$

The reverse saturation current density J_0 is temperature-dependent. It consists of diffusion current component $J_{0_{diff}}$ and recombination current component $J_{0_{rec}}$. When the device is biased at a low current level, the recombination mechanism dominates [8], [14], and J_0 can be simplified as:

$$J_0 = qWn_i/\tau_g \tag{3}$$

where W is the length of the depletion region, τ_g is the generation lifetime, n_i is the intrinsic concentration of the charge carriers. Here, n_i is equal to $(N_C N_V e^{-E_g/kT})^{0.5}$, where E_g is the bandgap of SiC, N_C, and N_V are the effective density of states of the conduction band and valence band edges, respectively. If N_C, N_V, W, and τ_g are taken as temperature-independent parameters as in [14], then the sensitivity of the temperature sensor can be expressed as:

$$S = \frac{dV_F}{dT} = \frac{nk}{q}\ln\left(\frac{I_{bias}\tau_g}{AqW}\right) - \frac{nk}{2q}\ln(N_C N_V) \tag{4}$$

Despite the temperature-dependency of E_g, there is no term containing E_g in the final expression, and therefore the change of SiC bandgap over temperature does not affect S.

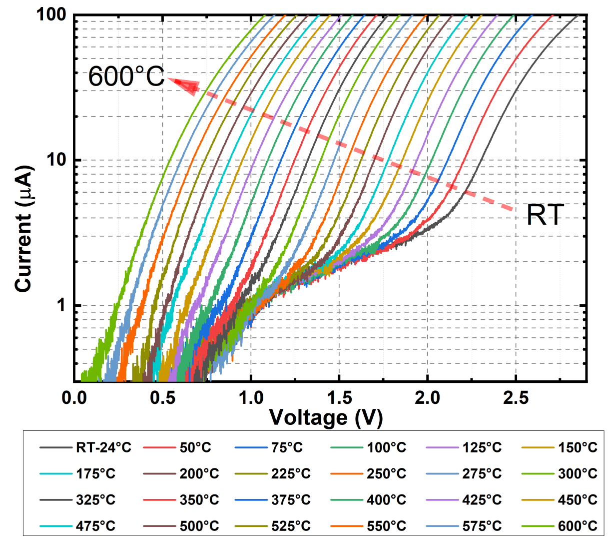

Fig. 3. The diode forward I-V_F curves at different temperatures were obtained by sweeping the voltage applied at the anode. As temperature increases, knee voltage of the diode decreases. When V_F increases, the diode becomes more ohmic due to series resistance.

B. Experimental Results

The diode was measured by the four-probe method with our dedicated high-temperature setup. During the measurement, the test chamber was pumped down to a high vacuum level (10^{-5} mbar) to minimize the oxidation of the probe tips and contact [17]. Before measurement at each temperature, a 15-minute waiting time was performed to ensure a stable temperature on the sample. Figure 3 is the I-V_F curve of the diode temperature sensor at different temperatures, ranging from room temperature to 600°C with steps of 25°C. Clearly, the sensor shows a typical diode-like I-V_F curve up to 600°C when V_F is small, i.e., the current increases exponentially as biasing voltage increases. As V_F further increases, the I-V_F curve becomes more linear since the series resistance starts to dominate the electrical behaviour. The ideality factor n can be extracted from the $(\ln I)$-V_F curve [9]. The ideality factor n is given as the following equation:

$$n = q/kT \cdot [dV_F/d(\ln I)] \tag{5}$$

The extracted ideality factor n shows a continuous decrease with respect to temperature rise, from 5.889 at room temperature to 2.067 at 600°C. The ideality factor at low temperatures is higher than the expected value, i.e., 2. Such a high ideality factor is a sign of deviation of the SiC diode from an ideal diode behavior at the low-temperature range. The non-ideality comes most probably from the poor p-type contact, as reported in [16]. To verify this, we measured the p- and n-type contact resistance by transmission line method (TLM) and extracted contact resistivity ρ_C, as summarized in Table I.

TABLE I
THE CONTACT RESISTIVITY OF n- AND p-TYPE MEASURED BY TLM

Contact type	Temperature (°C)	Contact resistivity ($\Omega \cdot cm^2$)
n-type	25	5.19×10^{-4}
n-type	600	8.38×10^{-4}
p-type	25	Schottky behavior
p-type	600	8.97×10^{-2}

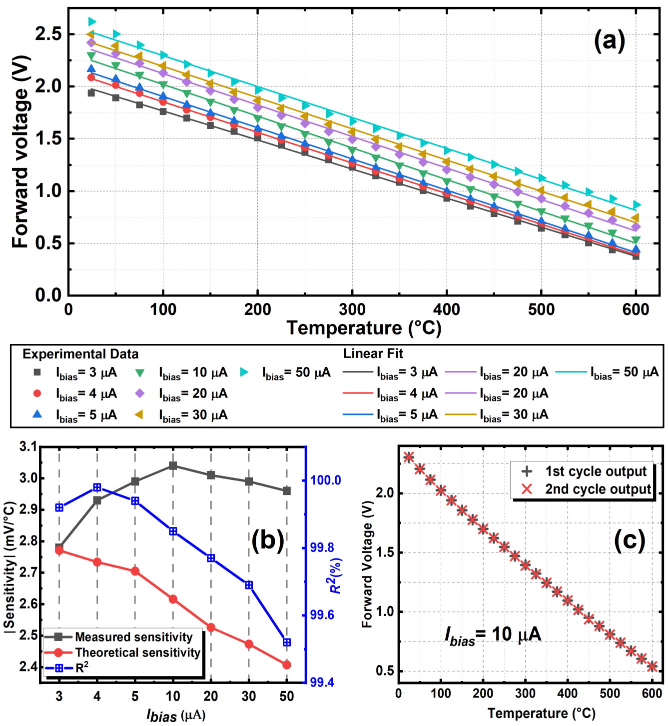

Fig. 4. (a) V_F vs. T when the p-n diode is biased at different current densities, ranging from 0.4 mA/cm^2 to 6.7 mA/cm^2. From room temperature to 600°C, the device shows fairly good sensitivity and linearity; (b) The measured sensitivity, theoretical sensitivity, and R^2 at different I_{bias}; (c) Sensor output under thermal cycles ($I_{bias} = 10$ μA).

Interestingly, the p-type contact showed Schottky properties at room temperature [18] and became ohmic at 600°C. The improved performance of p-type contact over temperature is the main contributor to the drop of n at high-temperature range. According to ρ_C, the diode contact resistance at the cathode and anode is estimated to be 139.67 Ω and 2650.71 Ω at 600°C. The reverse saturation current I_0 is extracted from the x-intercept of the linearly fitted $(\ln I)$-V_F curve. The saturation current increases with temperature from 18.2 pA at room temperature to 294.2 nA at 600°C. This can be attributed to the increase in n_i, more ionization of doping atoms, and an increase in the diffusion constant of the charge carrier as temperature increases [19]. From room temperature to 600°C, the number of ionized doping atoms in PW and SN increases from 1.52×10^{-16} to 9.62×10^{-16} atoms/cm^3 and from 3.53×10^{-18} to 1.44×10^{-19} atoms/cm^3, respectively [20].

Figure 4a demonstrates V_F versus temperature relation of the diode operating in the constant current forwards biasing (CCFB) mode. I_{bias} is kept small so that the charge carrier transport mechanism is recombination so that the assumption in (3) still holds [8], [14]. In our analysis, the linearity is evaluated by the coefficient of determination (R^2). From the fitting result, V_F shows a good degree of linearity ($R^2 > 99.5\%$) versus temperature under all biasing levels,

TABLE II
A SUMMARY OF SiC DIODE TEMPERATURE SENSOR REPORTED IN THE LITERATURE

Ref.	S (mV/°C)	R^2 (%)	Temperature range (°C)	Technology
[7]	3.30	99.96	175	Vertical Schottky
[8]	4.50	99.96	25-460	Vertical pin
[9]	2.66	99.99	25-300	Vertical pin
[10]	0.61	99.84	25-300	Vertical pin PTAT
[12]	1.18	99.97	-88-127	Vertical Schottky
[13]	2.70	/	25-550	Planar pin
[14]	3.50	/	25-600	Planar pn
This work	3.04	99.98	25-600	Planar pn in a SiC CMOS process

as shown in Figure 4b. Such a high degree of linearity introduces less error and reduces the calibration effort, which will ease the design of the readout circuit. The best linearity is obtained when $I_{bias} = 4$ μA, where R^2 is 99.98%. When $I_{bias} > 4$ μA, the linearity decreases as more voltage drop will be on the contact, which is not linear with temperature. If $I_{bias} < 4$ μA, then the linearity also becomes worse since the SiC diode might be still off because of low V_F.

The slope of the fitting curves indicates the sensitivity of the temperature sensor, which are close to each other under different current densities. With the best linearity, the sensitivity is -2.93 mV/°C ($I_{bias} = 4$ μA), thus the root mean square error (RMSE) of the temperature sensor is $\pm$ 0.47%. The maximum sensitivity is -3.04 mV/°C, which is obtained under a 10 μA biasing. Figure 4b also shows the theoretical sensitivity ($|S_{theory}|$) obtained from (4) compared to the experimental sensitivity ($|S_{measured}|$) at different biasing currents. Due to the transition from Schottky contact to ohmic contact over temperature, the voltage drop on the contact ($V_{contact}$) is expected to have a negative sensitivity to temperature ($S_{contact}$). As a result, $|S_{measured}|$ is generally larger than the predicted values. It can be also seen that $|S_{measured}|$ does not decrease monotonically as I_{bias} increases. The reason could be $S_{contact}$ is bias-dependent. At room temperature, $V_{contact}$ increases rapidly with I_{bias} until getting saturated at the knee voltage of the Schottky contact, translating to the same trend for $|S_{contact}|$. The summation of $|S_{contact}|$ and monotonically decreasing $|S_{theory}|$ eventually results in the general trend of $|S_{measured}|$ as shown in Figure 4b.

Figure 4c shows the sensor has a virtually identical response to repeated temperature profiles, indicating good repeatability from room temperature to 600°C. It is worth mentioning that the temperature range of this sensor is limited by the metallization as the Al interconnect starts to melt at 625°C. Despite this, our sensor can still outperform most SiC temperature sensors reported in the literature (summarized in Table II), not to mention its great potential in terms of monolithic integration.

IV. CONCLUSION AND FUTURE WORK

This work demonstrated a temperature sensor based on the SiC p-n diode, which is implemented in the FHG IISB's SiC CMOS technology. The temperature sensor is characterized in CCFB mode from room temperature to 600°C, showing a high linearity of up to 99.98% and a maximum sensitivity of 3.04 mV/°C. To our knowledge, this is the most linear diode-based temperature sensor with such a wide operating range. Continued optimization on the metal layer, long-term stability test, integration of the sensor with SiC ICs are planned.

References

[1] P. French, G. Krijnen, and F. Roozeboom, "Precision in harsh environments," *Microsyst. Nanoeng.*, vol. 2, no. 1, pp. 1–12, Oct. 2016.

[2] H.-P. Phan, D. V. Dao, K. Nakamura, S. Dimitrijev, and N.-T. Nguyen, "The piezoresistive effect of SiC for MEMS sensors at high temperatures: A review," *J. Microelectromech. Syst.*, vol. 24, no. 6, pp. 1663–1677, Dec. 2015.

[3] K. A. A. Makinwa, "Smart temperature sensors in standard CMOS," *Proc. Eng.*, vol. 5, pp. 930–939, Sep. 2010.

[4] K. A. A. Makinwa. *Temperature Sensor Performance Survey*. Accessed: Oct. 2018. [Online]. Available: http://ei.ewi.tudelft.nl/docs/TSensor_survey.xls

[5] C. van Vroohoven, D. D'Aquino, and K. Makinwa, "A ± 0.4 °C (3σ) -70 to 200 °C time-domain temperature sensor based on heat diffusion in Si and SiO_2," in *IEEE Int. Solid-State Circuits Conf. (ISSCC) Dig. Tech. Papers*, San Francisco, CA, USA, Feb. 2012, pp. 204–206.

[6] C.-M. Zetterling, "Integrated circuits in silicon carbide for high-temperature applications," *MRS Bull.*, vol. 40, no. 5, pp. 431–438, May 2015.

[7] V. Kumar, J. Verma, A. S. Maan, and J. Akhtar, "Epitaxial 4H–SiC based Schottky diode temperature sensors in ultra-low current range," *Vacuum*, vol. 182, Dec. 2020, Art. no. 109590.

[8] C. D. Matthus, T. Erlbacher, A. Hess, A. J. Bauer, and L. Frey, "Advanced 4H-SiC p-i-n diode as highly sensitive high-temperature sensor up to 460 °C," *IEEE Trans. Electron Devices*, vol. 64, no. 8, pp. 3399–3404, Aug. 2017.

[9] S. Rao, G. Pangallo, and F. G. D. Corte, "4H-SiC p-i-n diode as highly linear temperature sensor," *IEEE Trans. Electron Devices*, vol. 63, no. 1, pp. 414–418, Jan. 2016.

[10] S. Rao, G. Pangallo, and F. G. D. Corte, "Highly linear temperature sensor based on 4H-silicon carbide p-i-n diodes," *IEEE Electron Device Lett.*, vol. 36, no. 11, pp. 1205–1208, Nov. 2015.

[11] S. Rao, G. Pangallo, F. Pezzimenti, and F. G. D. Corte, "High-performance temperature sensor based on 4H-SiC Schottky diodes," *IEEE Electron Device Lett.*, vol. 36, no. 7, pp. 720–722, Jul. 2015.

[12] S. Rao, L. Di Benedetto, G. Pangallo, A. Rubino, S. Bellone, and F. G. D. Corte, "85–440 K temperature sensor based on a 4H-SiC Schottky diode," *IEEE Sensors J.*, vol. 16, no. 17, pp. 6537–6542, Sep. 2016.

[13] S. Hou, P.-E. Hellström, C.-M. Zetterling, and M. Östling, "4H-SiC PIN diode as high temperature multifunction sensor," *Mater. Sci. Forum*, vol. 897, pp. 630–633, May 2017.

[14] N. Zhang, C.-M. Lin, D. G. Senesky, and A. P. Pisano, "Temperature sensor based on 4H-silicon carbide pn diode operational from 20 °C to 600 °C," *Appl. Phys. Lett.*, vol. 104, no. 7, Feb. 2014, Art. no. 073504.

[15] T. Kimoto and J. A. Cooper, "Specialized silicon carbide devices and applications," in *Fundamentals of Silicon Carbide Technology: Growth, Characterization, Devices and Applications*, 1st ed. Singapore: Wiley, 2014, pp. 487–510.

[16] J. Romijn, S. Vollebregt, L. M. Middelburg, B. E. Mansouri, H. W. van Zeijl, A. May, T. Erlbacher, G. Zhang, and P. M. Sarro, "Integrated digital and analog circuit blocks in a scalable silicon carbide CMOS technology," *IEEE Trans. Electron Devices*, vol. 69, no. 1, pp. 4–10, Jan. 2022.

[17] M. Masunaga, V. Crescitelli, and T. Funaki, "Long-term stability of nickel-based ohmic contacts with n-type and p-type 4H-SiC in a high-temperature environment," *Jpn. J. Appl. Phys.*, vol. 59, no. 10, pp. 104005-1–104005-8, Oct. 2020.

[18] A. May, M. Rommel, S. Beuer, and T. Erlbacher, "Via size-dependent properties of TiAl ohmic contacts on 4H-SiC," *Mater. Sci. Forum*, vol. 1062, pp. 185–189, May 2022.

[19] M. Badila, J. P. Chante, M. L. Locatelli, J. Millan, P. Godignon, G. Brezeanu, B. Tudor, and A. Lebedev, "Temperature behavior of the 6H-SiC pn diodes," *Diamond Rel. Mater.*, vol. 8, nos. 2–5, pp. 341–345, Mar. 1999.

[20] R. F. Pierret, "Equilibrium carrier statistics," in *Advanced Semiconductor Fundamentals*, vol. 6, 2nd ed. Boston, MA, USA: Addison-Wesley, 1987, pp. 87–128.